Mechanics and mechanisms of magmatic underplating: inferences from mafic veins in deep crustal mylonite

M.R. Handy [a,*], J.E. Streit [b]

[a] *Institut für Geowissenschaften, Justus-Liebig Universität Giessen, Senckenbergstrasse 3, D-35390 Giessen, Germany*
[b] *Department of Geology, Australian National University, Canberra ACT 0200, Australia*

Abstract

Dioritic to gabbro–dioritic veins with extreme length to width ratios (>1000 : 1) are localized along an amphibolite facies shear zone (the CMB Line) between exposed segments of originally middle and lower continental crust (Strona–Ceneri and Ivrea–Verbano Zones, northern Italy). The geometry of these veins and their mutual cross-cutting relationships with the mylonitic foliation indicate that veining was coeval with noncoaxial flattening of the lower crust in Early Permian time. The veins formed as closely spaced extensional shear fractures and propagated parallel to the originally gently to moderately dipping ($\leq 30°$) mylonitic foliation. Vein opening at high angles (60–90°) to the inferred σ_1 direction and subparallel to the pre-existing planar fabric requires that melt pressure slightly exceeded the lithostatic pressure and that differential stress was low (≤ 10–20 MPa) in the vicinity of the veins. The interaction of regions of tensile stress concentration at vein tips caused the concordant veins to curve and link up across the mylonitic foliation. Once interconnected, the veins served as conduits for the rapid movement of mafic melt along the shear zone. Thermal modelling constrains the mafic melt in the narrowest, 1 mm wide veins to have crystallized almost instantaneously. Such veins extend no more than a meter from host veins into the country rock, indicating that the minimum rate of vein tip propagation and melt flow was at least several m/s. Maximum crystallization times of only hundreds to thousands of years for even the thickest mafic veins (10–100 m) in the IVZ are short compared to the 15–20 Ma duration of Early Permian crustal attenuation and magmatism in the southern Alps. This suggests that veining in the lower crust occurred episodically during extended periods of mylonitic creep. Concordant vein networks within deep crustal shear zones that are inclined (as the CMB Line may have been) can also channel overpressurized mafic melt from deeper sources, e.g. lower crustal magma chambers, into cooler, intermediate crustal rock. This locally widens the depth interval of combined viscous and brittle deformation within the crust and can trigger partial melting of the country rock. © 1999 Elsevier Science B.V. All rights reserved.

Keywords: magmas; underplating; shear zones; brittle materials; viscous materials; mylonites

1. Introduction

Magmatic underplating plays an important role in forming and transforming the continental crust [1], yet the mechanisms by which large volumes of mantle-derived melt are emplaced within the lower crust remain enigmatic. Debate centers on two interrelated questions: (1) Was the melt originally emplaced as dikes or as sills? and (2) Do melt layers pre-, syn- or post-date deformation of the lower crust? Laterally continuous zones of enhanced con-

---

ductivity and seismic reflectivity within the lower crust of intracontinental rifts [2], passive continental margins [3] and thinned orogenic continental crust [4] are often attributed to subhorizontal laminae of dense mafic rock or melt within felsic granulites [5,6]. Some workers [7] have speculated that the subhorizontal attitude of these laminae is not primary, but resulted from pervasive shearing and rotation of dikes during lateral crustal attenuation. More recently, others have proposed that overpressurized mafic magmas can intrude the crust as dikes or sills depending on the melt pressure and viscous strength of the rheologically stratified lithosphere [8]. Numerical fracture propagation models support the notion that dikes serve as conduits for the rapid ascent of large volumes of granitic melt [9,10]. Melt migration without fracturing of the rock has been invoked for some migmatites where leucosome is observed to collect in boudin necks [11]. However, layer-parallel leucosome or magma intrusions in migmatitic terranes are often associated with fracturing at high melt pressures [11,12].

This paper presents field evidence that magmatic underplating involves the intrusion and linkage of thin, long mafic veins along active mylonitic shear zones. We show how existing failure criteria applied to the geometry of these veins provide constraints on both the differential stress and melt pressure at the time of intrusion, and how consideration of vein tip stresses allow the evolution of the vein array to be reconstructed. Finally, we speculate on how mantle-derived melts interact with large shear zones and condition both the structure and rheology of the continental crust.

2. Geological setting

Mafic veins are localized within an amphibolite facies mylonite belt, the so-called CMB Line (CMB = Cossato–Mergozzo–Brissago Line [13]), that forms the subvertically dipping tectonic contact between the lower crustal Ivrea–Verbano Zone (IVZ) and intermediate crustal Strona–Ceneri Zone (SCZ) of the southern Alps (Fig. 1). The mylonites of the CMB Line are derived from high grade gneisses and schists of these two Zones and contain the syn-kinematically stable mineral parage-

nesis quartz–plagioclase–biotite–muscovite–garnet–sillimanite (fibrolite). We refer to the deformed rocks of the CMB Line as 'mylonites' or 'mylonitic' because they are foliated and, in thin section, contain microstructural evidence that the mineral which accommodated most of the bulk strain (in this case, quartz) underwent complete dynamic recovery and recrystallization. Mylonitization along the CMB Line is actually related to amphibolite to granulite facies mylonitic shear that affected much of the IVZ and the northernmost part of the SCZ in Early Permian time [14]. This deformation coincided with the intrusion of large volumes of gabbroic, gabbro–dioritic and ultramafic magmas in the originally deepest parts of the exposed crustal section, presently exposed in the northwestern part of the IVZ (Fig. 1; [15] and references therein). Early Permian magmatic underplating is temporally related to granitic and rhyolitic magmatism in originally shallower levels of the southern Alpine crust [16], and probably occurred during regional transtensional tectonics [17].

At this point, we emphasize two aspects of the local geology that bear directly on this study of syn-mylonitic veining: (1) the basement containing the CMB Line north of the Lago Maggiore (Fig. 1) does not occupy its original, Early Permian orientation, but was rotated at least 60º into its present subvertical attitude during Tertiary Insubric faulting and folding [18]. Paleomagnetic and structural studies in the area indicate that prior to Alpine orogenesis, the mylonitic foliation within the IVZ and along the CMB Line was inclined 30º or less to the southeast ([14] and references therein). The CMB mylonites are therefore interpreted to be the deeply eroded part of an oblique-extensional shear zone that, prior to Alpine differential rotation and erosion, was linked to steep faults bounding Early Permian basins in the upper crust of the southern Alps [14]. The originally shallow dip of the mylonitic foliation along the CMB Line becomes important below when discussing the Early Permian kinematic regime and stress field in the vicinity of the mafic veins. (2) The central segment of the CMB Line as well as the narrow, northeastern part of the IVZ (north of Lago Maggiore in Fig. 1) is overprinted by Early Mesozoic, retrograde amphibolite to greenschist facies mylonites of the Pogallo Line [17]. We obviously avoided these
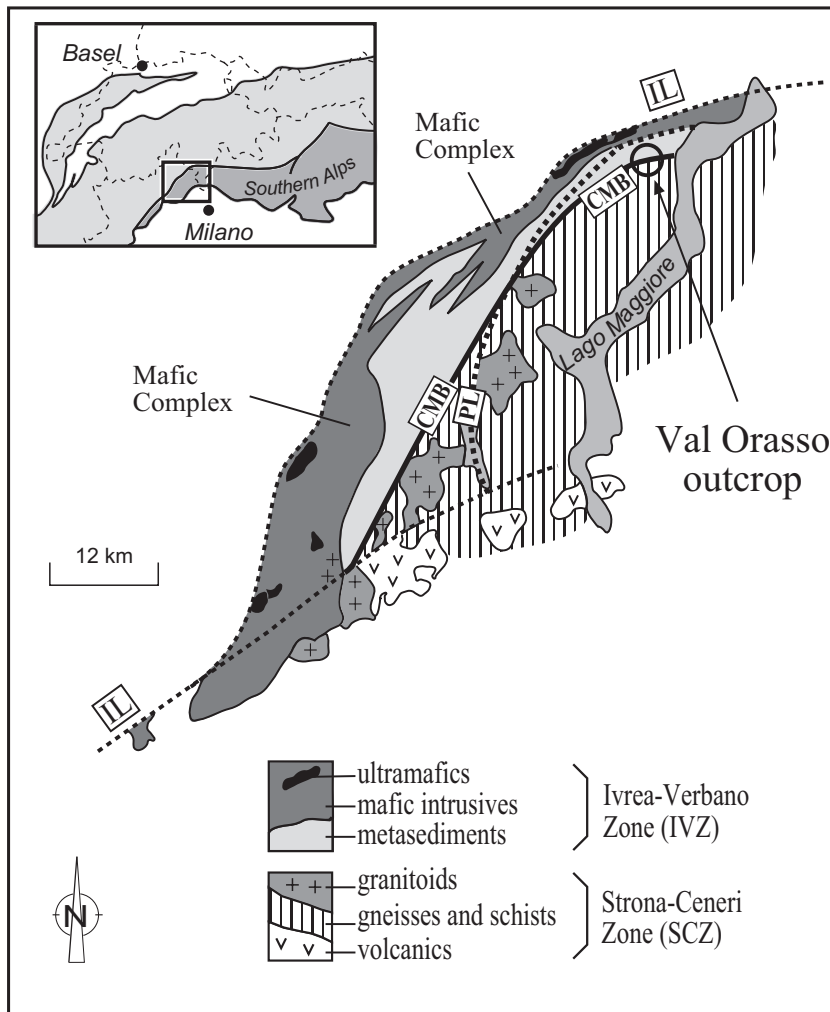
Fig. 1. General map of the Ivrea crustal cross section showing location of the CMB Line (*CMB*) forming the contact between the Ivrea–Verbano and Strona–Ceneri Zones in the Southern Alps. *PL* = Pogallo Line, *IL* = Insubric Line. Details of Val Orasso outcrop shown in Figs. 2 and 3.

areas because of the modifying effect this later deformation had on the primary geometry of the mafic veins.

3. Vein–mylonite relations

For the purposes of this study, we restricted detailed investigations to a well exposed outcrop in the stream bed of the Orasso valley that runs parallel to the strike of the subvertical mylonitic foliation (S_m) and mafic veins of the CMB Line (Fig. 2). The veins

along the CMB Line are dioritic to locally gabbro–dioritic and comprise mostly magmatic plagioclase and hornblende with rare inclusions of clinopyroxene [13]. The hornblende is partly transformed to metamorphic biotite in fully mylonitized veins and at the rims of deformed veins. The primary mineralogy of the veins is virtually identical to that of Early Permian gabbro–diorites of the Mafic Complex in the Ivrea Zone [19,20] and their main and trace element chemical compositions clearly manifest an upper mantle heritage [16,21].

The most striking features of the mafic veins are
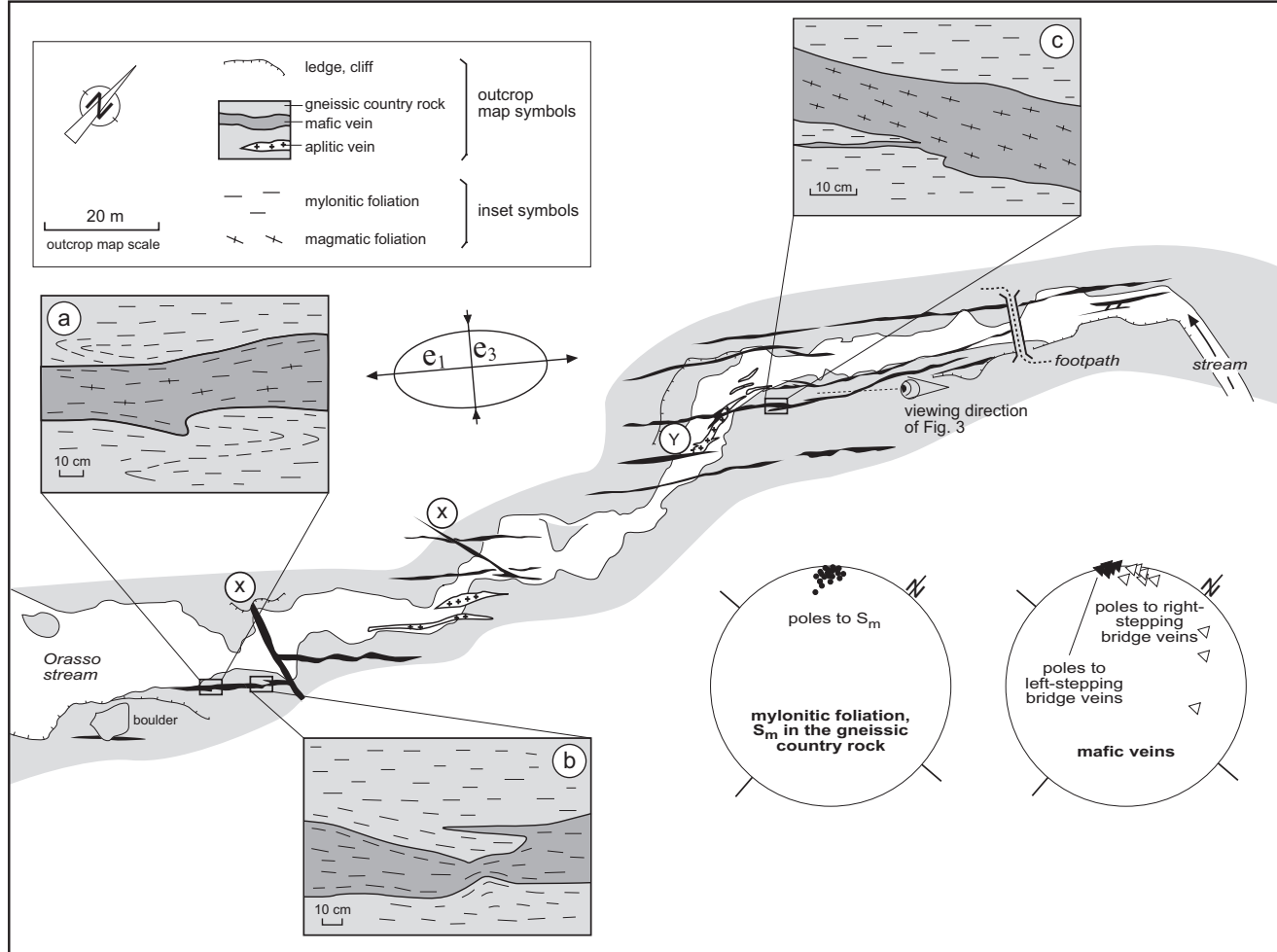
Fig. 2. Outcrop map of syn-mylonitic mafic veins along the CMB Line. Map view is approximately parallel to the XZ fabric plane, as indicated by the orientation of the e_1e_3 finite strain ellipse. Inset sketches: (a) local jog of vein margin; (b) neck in right-leaning bridge vein connecting the ends of a pair of left-stepping concordant veins; (c) left-leaning bridge vein with concordant veinlet and locally discordant jog along lower margin (see also Fig. 3c); discordant veins labelled X and Y are described in text. Eyeball symbol looks in direction of view in Fig. 3a. Equal area plots (lower hemisphere) show measured orientations of S_m and bridge veins (see text).

their high length to width ratios ($>1000:1$) and their locally irregular orientation with respect to the mylonitic foliation (Figs. 2 and 3a). Long concordant veins are linked by right- and left-leaning bridge veins that truncate S_m at 10 to 20° (equal area plots in Figs. 2 and 3b). In rare instances, mafic veins cut across both S_m and concordant veins at moderate to high angles (locations marked 'X' in Fig. 2). These discordant veins show evidence for combined extension and dextral displacement parallel to their margins. Most, but not all, of the veins truncate sigmoidal extensional veins and pull-apart structures filled with aplite (location 'Y' in Fig. 2).

The discordant bridge veins are asymmetrically developed (Fig. 2b,c): The convex sides of these veins contain one or more barbs that taper away from the vein within the S_m, whereas the concave sides of the bridge veins are smoothly arcuate and only locally contain discordant jogs. The minor amount of deformation within bridge veins linking adjacent concordant veins (Fig. 2b) indicates that the veins did not significantly rotate into the foliation during mylonitization and therefore that their concordant orientation is primary.

The following features indicate that mafic veining was broadly coeval with mylonitization: Some veins are undeformed and show primary magmatic structures (e.g., chilled margins: Fig. 3b,c; oriented phenocrysts in a magmatic fabric: Fig. 3d), whereas others are boudinaged and show a solid-state mylonitic overprint along their margins (inset Fig. 2a,b). Yet other veins are completely mylonitized and have been transformed to fine grained biotite–amphibole layers parallel to the mylonitic foliation (Fig. 3b). The spatial coexistence of mafic veins that both cut, and are deformed by, the same mylonitic foliation in the country rock is diagnostic of syn-kinematic veining. The fact that some of the mafic veins are only slightly deformed indicates that veining continued until the end of mylonitization.

The relatively greater stretch of boudinaged veins in map view in Fig. 2 than in outcrop surfaces perpendicular to this view indicates that the direction of greatest finite strain, e_1, is horizontal within the subvertical S_m plane. Mylonitization involved a strong component of shortening subperpendicular to S_m, as manifest by the pinch-and-swell structure of deformed mafic veins in mutually perpendicular

directions within S_m and by the lack of a well-defined stretching lineation. In addition, a component of sinistral noncoaxial shear subparallel to S_m is inferred from the prevalence of southwest-facing isoclinal folds in the mylonitic country rock, the right-stepping asymmetrical tails of sigma-shaped quartzo-feldspathic augen, and the minor sinistral offset of discordant pegmatitic dikes along discrete microshears parallel to S_m. The presence of chilled margins at either end of concordant veins viewed in the XZ fabric plane suggests that the vein tips propagated in opposite directions within the mylonitic foliation and that the melt therefore intruded from the intermediate principal strain direction.

The dioritic melt in the veins was just below the liquidus at the time of intrusion judging from the massive, magmatic fabric surrounding rare, hornblende phenocrysts that are preferentially oriented subparallel to the vein margins (e.g., Fig. 3d). The liquidus temperature is poorly constrained, but was definitely higher than a temperature of about 800–1000°C for melt containing hornblende and plagioclase in the absence of garnet in amphibole melting experiments [22]. An intrusive temperature greater than 1000°C is inferred from the occurrence of chilled margins in the veins (Fig. 3b) and from evidence that the mafic veins were sufficiently hot to induce syn-mylonitic partial melting of the country rock in their vicinity (e.g., leucosomes in intrafoliational boudin-necks and pull-apart structures). Simultaneous mafic veining and partial melting of the deforming country rock is further documented by leucocratic veins filled with anatectic melt from the country rock that intruded and brecciated the mafic veins. Anatectic back-veining and brecciation of the mafic veins indicates that the mafic melt cooled rapidly enough to have acquired a fracture strength during partial melting and mylonitization of the country rock.

Cation-exchange geothermometry and geobarometry on contacting metamorphic minerals in the country rock yield temperatures and lithostatic pressures adjacent to the veins in the range of 650–750°C and 300–550 MPa [23]. However, these probably represent retrograde conditions rather than the peak temperature and pressure at the time of intrusion. An upper limit of about 600–700 MPa for the lithostatic pressure during intrusion is indicated by
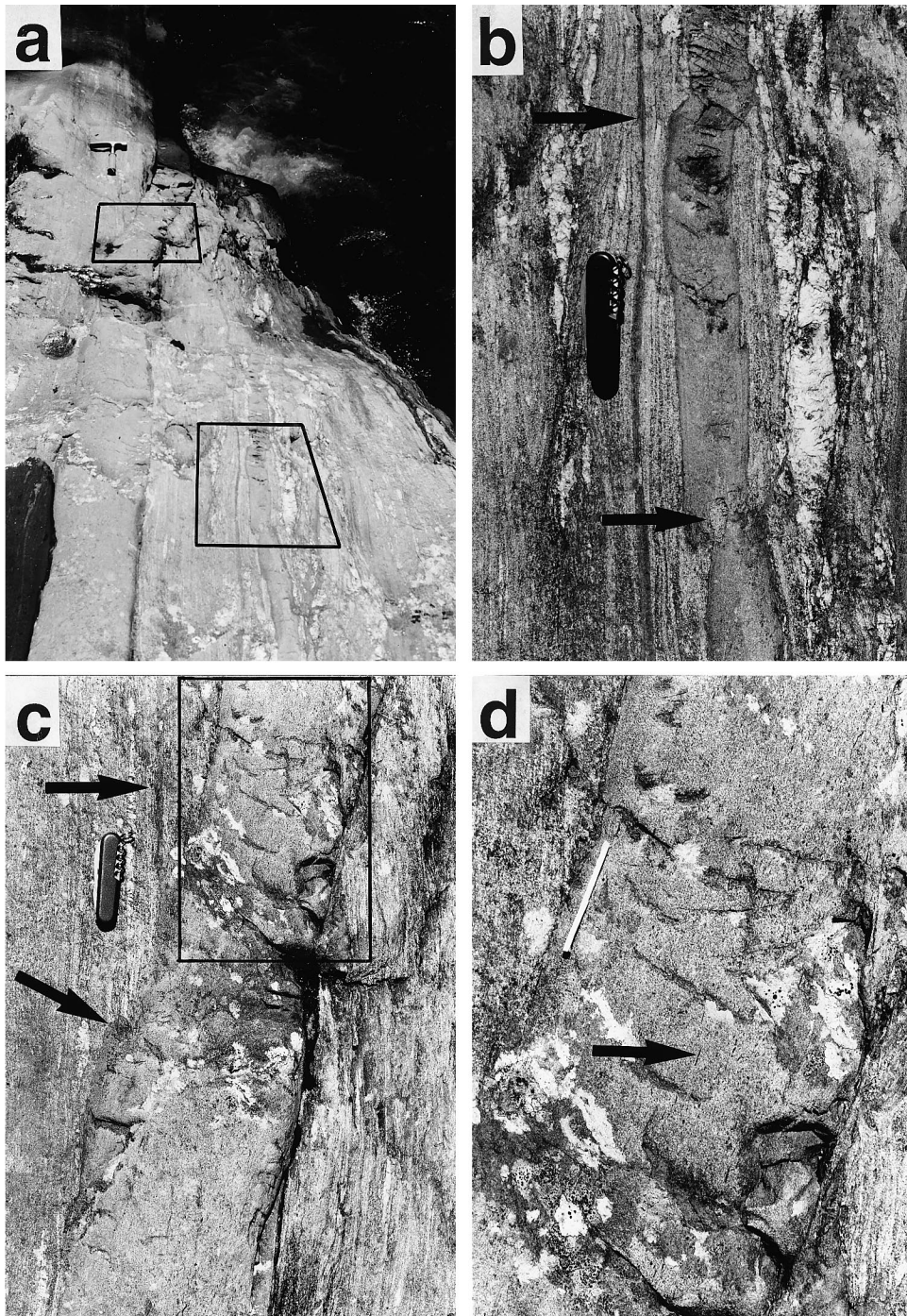
Fig. 3. Mafic vein geometry: (a) Sinuous mafic vein viewed along its length subparallel to S_m (boxed areas shown in (b), (c)); (b) Concordant vein with dark chilled margins shows right- and left-leaning bridges and rounded xenolith of mylonitic country rock (lower arrow); note the completely mylonitized vein (upper arrow) within S_m of the country rock; (c) Left-leaning bridge vein segment with jog (lower arrow) and veinlet parallel to S_m (upper arrow) both emanating from the same margin, boxed area shown in (d); (d) Detail of (c) showing chilled margins and magmatic foliation defined by hornblende phenocrysts (arrow points to one example).

comparison of the aforementioned solid phases in the mafic veins with phase stabilities in amphibole melting experiments [22]. This pressure range corresponds to an intrusive depth range of 21–27 km if one assumes average crustal densities of 2.7–2.8 g cm^{-3} for granitoid to mafic continental crust.

4. Constraints on differential stress and melt pressure during veining

As mentioned above, the presently subvertical mylonitic foliation and mafic veins along the CMB Line originally dipped 30° or less to the southeast. Accordingly, the direction of greatest finite shortening, e_3, plunged 60 to 90° at the time of synmylonitic intrusion. Given the strong coaxial component of deformation, we infer that the e_3 direction (Fig. 2) was close to the direction of maximum principal stress, σ_1. Therefore, the angle θ between σ_1 and S_m and, thus, between σ_1 and the concordant veins (inset to Fig. 4a) must have been close to 90° within the range 45° < θ < 90°.

The orientation of mafic veins at such high angles to σ_1 is an unfavorable fracture orientation in isotropic rock [24] and suggests that the pre-existing mylonitic foliation rendered the country rock mechanically anisotropic during veining. Specifically, the tensile strength of the mylonite normal to the foliation, T_n, must have been much less than that at other angles to the foliation, T_{tr} (the subscript tr denotes tensile strength 'through the rock'). The dependence of rock strength on the orientation of foliation with respect to the principal stress axes is well documented in triaxial experiments on metamorphic rocks and is evident from the opening of hydrofractures in foliated crustal rocks [25,26] and of granitoid veins in partially melted gneisses [12] at high angles to σ_1. The effect of foliation on rock strength is depicted in Fig. 4a in a Mohr diagram containing two failure envelopes, one for fracturing parallel to S_m (labelled ∥ foliation) and another for failure at all other angles (labelled 'tr'). Also included is a horizontal envelope for viscous flow of mylonite at a constant natural strain rate. This envelope is tangent to a Mohr circle representing the stress state in the mylonitic country rock away from the mafic veins (see discussion below).

The discussion below is based on the Law of Effective Stress (i.e., Terzaghi's Law) which states that the pressure of fluids in a rock reduces the normal stress on a fault plane in that rock. We distinguish between the pressure of metamorphic fluids, P_f, and the pressure of melts, P_m. Although melts usually have different viscosities and wetting angles than metamorphic fluids, they are mechanically similar in that they exert isotropic (i.e. non-directional) pressure. We emphasize that the melt pressure in propagating cracks and veins exceeds the pressure of presumably aqueous fluid in the pore space of intact, mylonitic country rock. In contrast to pore fluids (e.g., aqueous fluids in metamorphic rocks or leucosome in migmatitic rocks) in partly connected pore space, mafic melt is only connected along macroscopic fracture networks. In the following, we show how the distribution of these different fluids can be used to constrain the stress state in the deep, anatectic crust.

The differential stress in the mylonite is poorly constrained, but purely extensional aplitic veins in the mylonite (marked 'Y' in Fig. 2) indicate that, at least transiently and locally within the mylonite, $\Delta\sigma \leq 4T_{tr}$ and $P_m \geq \sigma_3 + T_{tr}$ [27,28]. Taking an average value of 10 MPa for the laboratory tensile strength of basement rocks [28], one can estimate that the differential stress in the mylonite during aplitic veining did not exceed 40 MPa. The effective lithostatic pressure in the mylonite was about 60–70 MPa, a value obtained from the maximum lithostatic pressure (600–700 MPa) and an assumed average pore fluid factor $\lambda = 0.9$ (λ = pore fluid pressure/lithostatic pressure). An aqueous pore fluid is assumed to occupy the pore space of the mica-rich mylonites. Near lithostatic fluid pressure is reasonable for such fluids in aggregates undergoing dynamic recrystallization in the deep crust [29,30]. In view of the poor constraints on the original orientation of the mylonitic foliation, we assume that the effective lithostatic pressure (P_1') is approximately equal to the effective mean stress ($\sigma_m' = (\sigma_1 + \sigma_3)/2 - P_f$). The effective mean stress is the locus of the center of the Mohr circle along the normal stress axis in Fig. 4a.

For mafic veins to propagate within the mylonitic foliation at high angles to the σ_1 direction, the stress state near the veins must have differed from that
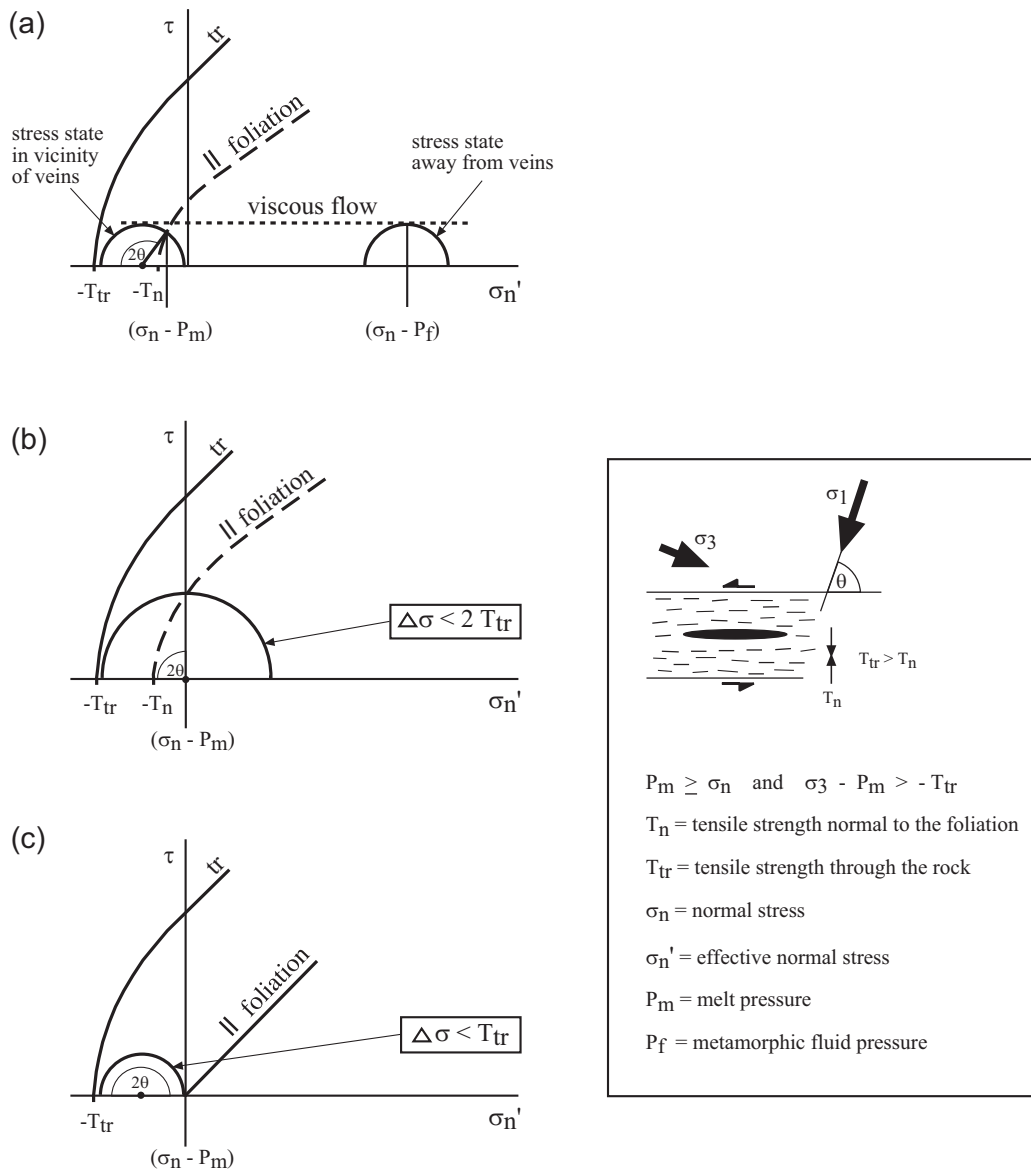
Fig. 4. Mohr diagrams with Griffith and Navier–Coulomb failure envelopes representing the strength of mylonites in planes parallel to the foliation (|| foliation) and in all other directions (tr): (a) Mohr diagram depicting stress state for failure in extensional shear parallel to the foliation at $45° < \theta < 90°$. The horizontal envelope represents the creep strength of the country rock at the local strain rate. The sketch illustrates the inferred orientation of the principal stress axes with respect to a mafic vein (black) and foliation (thin lines), as viewed in the XZ fabric plane (map view in Fig. 2); (b) Mohr circle representing maximum differential stress for failure at $\theta = 45°$ and $\sigma_n - P_m = 0$; (c) Mohr circle representing maximum differential stress for a vein opening at $\theta = 90°$ and $\sigma_n - P_m = 0$ (see text for explanation). The failure envelopes in (a) and (b) for the strength of mylonite in planes parallel to the foliation are dashed because these envelopes do not exist any longer at that location in the rock once the fracture has formed.

away from the veins in the mylonitic country rock. The differential stress in the mylonite adjacent to the veins and the melt pressure within the veins are constrained mainly by two factors: (1) the magnitude of the strength anisotropy of the mylonite (i.e., the distance between the failure envelopes in Fig. 4);

and (2) the angle θ between the inferred σ_1 direction and S_m. The fact that the mafic veins opened at high angles ($45° < \theta < 90°$) to σ_1 indicates that the melt pressure, P_m, not only exceeded σ_3, but was equal to or greater than the normal stress σ_n, on S_m (Fig. 4a). Failure parallel to the foliation at zero or negative effective normal stresses, σ'_n, on S_m requires very small differential stresses in the absence of evidence for failure through the rock in shear or tension. The range of possible stress states corresponding to this condition can be depicted as a family of Mohr circles (one of which is shown in Fig. 4a) whose position and radii along the effective normal stress axis allow them to intersect the parallel-to-foliation failure envelope at $90° < 2\theta < 180°$ without touching the through-the-rock failure envelope. We emphasize that the intersection of the stress circles in Fig. 4 with the parallel-to-foliation failure envelope predicts failure along the foliation only at the specific, non-optimal angle θ (depicted as 2θ in Mohr diagrams) between σ_1 and the foliation.

Because the original dip of the mylonitic foliation, the orientation of the principal stresses, and the magnitude of anisotropy in mylonite strength are all poorly constrained, we can only estimate a range of maximum differential stresses and melt pressures that prevailed, respectively, adjacent to and within the concordant veins. We do this in the following way: For fracture angles (i.e., the angle θ between σ_1 and the fracture surface) of $\theta \geq 45°$ at negative or zero effective normal stresses on the mylonitic foliation (Fig. 4a), the mean stress must have been zero or negative. Accordingly, the differential stress for failure along the mylonitic foliation without causing failure through the rock in shear or tension is limited by the expression:

$$\Delta\sigma < 2T_{tr} \tag{1}$$

Fig. 4b depicts the conditions at which the differential stress in expression (1) approaches a maximum value of $2T_{tr}$ at the fracture angle $\theta = 45°$ (concordant vein opening at 45° to the σ_1 direction). If, on the other hand, one assumes the maximum θ value of 90° (concordant vein opening in the σ_1 direction), the largest possible differential stress is attained for zero tensile strength normal to the foliation, as depicted in Fig. 4c. This maximum differential stress must have been less than the tensile strength through the rock

(Fig. 4c), corresponding to the limiting relation:

$$\Delta\sigma < T_{tr} \tag{2}$$

By substituting the previously cited average value of 10 MPa for the laboratory tensile strength of intact isotropic rock [28] in the expressions above, we constrain the maximum differential stress near the concordant veins to have been less than 20 to 10 MPa, respectively, for the minimum (45°) and maximum (90°) values of θ. Maximum values close to 10 MPa are more reasonable given the structural evidence above for shortening subperpendicular to the mylonitic foliation.

This maximum differential stress estimate falls well within the range of differential stresses predicted from the extrapolation of experimentally derived, power law creep equations [31] to the natural creep rates and temperatures of mylonitization in the gneisses of the Orasso outcrop. The Mohr circles for simultaneous magma veining and mylonitic flow in Fig. 4a are therefore drawn with the same radii.

There is evidence that the stress state within the outcrop varied considerably during veining. For example, two highly discordant veins labelled 'X' in the outcrop map (Fig. 2) truncate concordant veins and show clear evidence of combined extension and dextral shear along their boundaries. The differential stress must have slightly exceeded that required for pure extensional failure through the rock (40 MPa, see above) in order to account for our observation of hybrid extensional-shear failure [27].

To estimate the melt pressure (P_m) during concordant veining, we assume that the effective normal stress (σ'_n) on the originally moderately to shallowly dipping mylonitic foliation was equal to the effective lithostatic pressure (P'_l), which is constrained by $\sigma'_1 \leq P'_l \leq \sigma'_3$. Because the differential stress ($\sigma'_1 - \sigma'_3$) during veining was very small (<20 MPa) and the effective normal stress was zero or slightly negative (Fig. 4), the deviation of σ'_n from P'_l was less than the tensile strength of intact rock (<10 MPa). For zero or slightly negative effective normal stress about equal to the effective lithostatic pressure ($\sigma'_n \approx 0 \approx P_l - P_m$), the minimum melt pressure was approximately 600–700 MPa, equivalent to the maximum lithostatic pressures (600–700 MPa) derived above from the magmatic mineral assemblage in the veins.

5. Geometry and evolution of the mafic veins

The bridge veins linking the concordant mafic veins (Fig. 3a) lend a sinuous geometry to the overall vein array (Fig. 2). This geometry is interpreted to reflect the interaction of tensile stress concentration fields at the tips of closely spaced veins. Such interactions are well documented in experimentally stressed, flawed materials and so the model of vein evolution presented below and in Fig. 5 is based partly on analogies with these experiments and with crack theory.

During a first stage, mafic melt migrated along the mylonitic foliation in narrowly spaced, highly pressurized, extensional shear cracks (Fig. 5a). The geometry of the tensile stress concentration fields at the crack tips governed the way in which these veins eventually interconnected. This geometry can be reconstructed from the following considerations: The tips of internally pressurized, mode 1 (extensional) cracks are associated with tensile stress concentration fields that are heart-shaped and symmetrically distributed about the tip ([32]: their Fig. 5). In contrast, the tips of mode 2 (shear) cracks have both tensile and compressional stress concentration fields that form asymmetrically distributed lobes at opposite ends and sides of the crack tips ([33]: their fig. 8.7B). Unlike these two end-member configurations, however, the mafic veins in the CMB mylonites opened as internally pressurized, mixed mode 1 and 2 fractures, with σ_1 oriented at a high angle to the mechanical anisotropy, S_m. The tensile stress concentration fields at tips of the mafic veins (stippled areas in Fig. 5a) are therefore inferred to form slightly asymmetrical lobes, with larger lobes at opposite ends and sides of the cracks skewed in the direction of the remote σ_1.

During Stage 2, tensile stress concentration fields at the tips of closely spaced, concordant veins propagating in opposite directions began to overlap (Fig. 5b). This induced one or both of the vein tips to curve toward and intersect the side of the nearest vein propagating in the opposite direction. Such 'tip-to-plane' propagation through interacting tensile stress fields [34] has been invoked to explain the interconnection and sigmoidal shape of en échelon veins in isotropic and weakly compressive stress fields where σ_1 lay in the plane of pre-existing
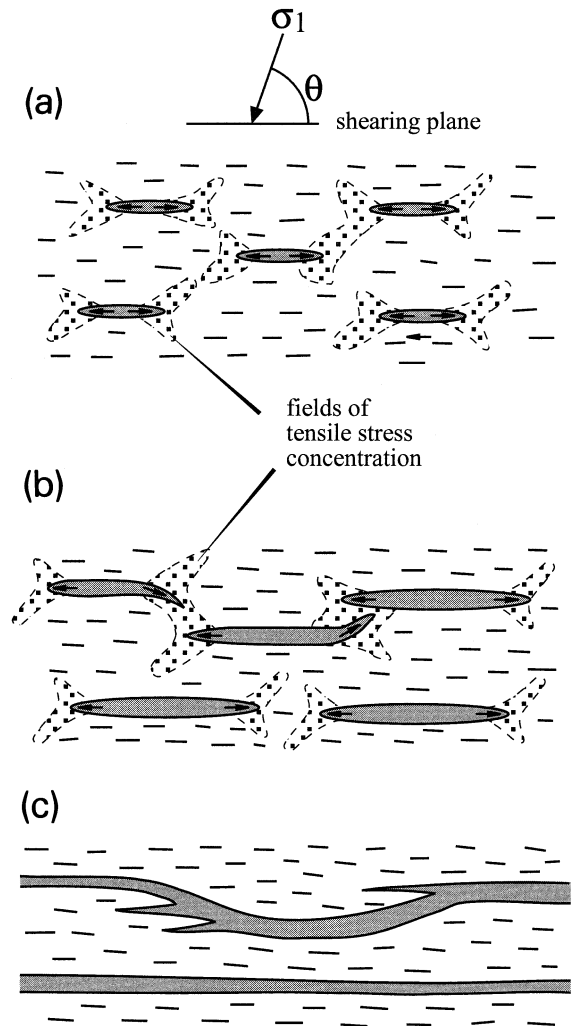
Fig. 5. Sketch of evolution of overpressurized mafic veins as viewed in the XZ fabric plane (map view in Fig. 2): (a) Propagation of extensional shear veins parallel to S_m (Stage 1); (b) Tip-to-plane curvature of veins due to interaction of tensile stress fields at the vein tips (Stage 2); (c) Linked veins form interconnected melt pathways along the shear zone. In (a) and (b), stippled areas bounded by dashed lines indicate tensile stress fields, small arrows within veins depict direction of tip propagation.

mode 1 cracks [32,35]. The same mechanism has also been proposed for the arcuation of tensile cracks between mode 2 cracks in rocks [36] and rock-analogue materials [37] subjected experimentally to simple shear (σ_1 at 45° to cracks). The bridge cracks extending from and linking the pre-existing planar

cracks in these experiments were planar to arcuate (e.g., [34]: their figs. 13, 14; [38]: "wing cracks" in their figs. 4, 13), as observed in the bridge veins of the Orasso outcrop. The bridge cracks in the simple shear experiments lean in a direction opposite to the stepping-direction of their planar host cracks ([36]: their fig. 6). By analogy with these experiments, the interaction of tensile stress fields at the tips of pressurized, concordant mafic veins in mylonite that accommodates a large component of flattening sub-perpendicular to the foliation should engender bridge veins leaning in conjugate directions with respect to the concordant veins. The tip-to-plane propagation directions and bridge veins depicted in Fig. 5b,c are drawn to reflect this expectation.

The intrusion and linkage of the mafic veins occurred in short bursts during mylonitization because only one generation of chilled margins is observed within the veins. The veins are narrow (<50 cm wide), and the temperature contrast between veins and surrounding mylonitic gneiss was large ($\Delta T = 200$–400°C). Using a simple half-space conductive cooling and crystallization model ([39]: chapt. 4–18), one can predict maximum crystallization times

ranging from just over 3 days for the widest veins (50 cm) to only about 1 second for the narrowest (1 mm) veins (Fig. 6). A rapid increase in melt viscosity during such short crystallization times probably explains why only veins with widths greater than 5 cm are observed to have propagated for distances longer than a few meters. The narrowest veins (e.g., thin concordant vein emanating from the outer margin of the discordant bridge vein in Fig. 2c and Fig. 3c) crystallized so quickly that they could intrude no further than a meter into the gneiss. As fracture propagation was driven by the overpressured melt, the maximum crystallization time of about 1 second for the longest ($\sim$1 m) of the narrowest ($\sim$1 mm) veins also places an absolute lower limit of about 1 m/s on the vein tip propagation rate. As this minimum rate is two orders of magnitude greater than even the highest laboratory propagation rates for subcritical cracks [40], it is reasonable to assume that the vein tips propagated critically at rates approaching the speed of shear waves in rock [40].

The model above explains some of the enigmatic vein structures described in Section 3 and in other occurrences of syn-mylonitic, mafic veins [41,42].
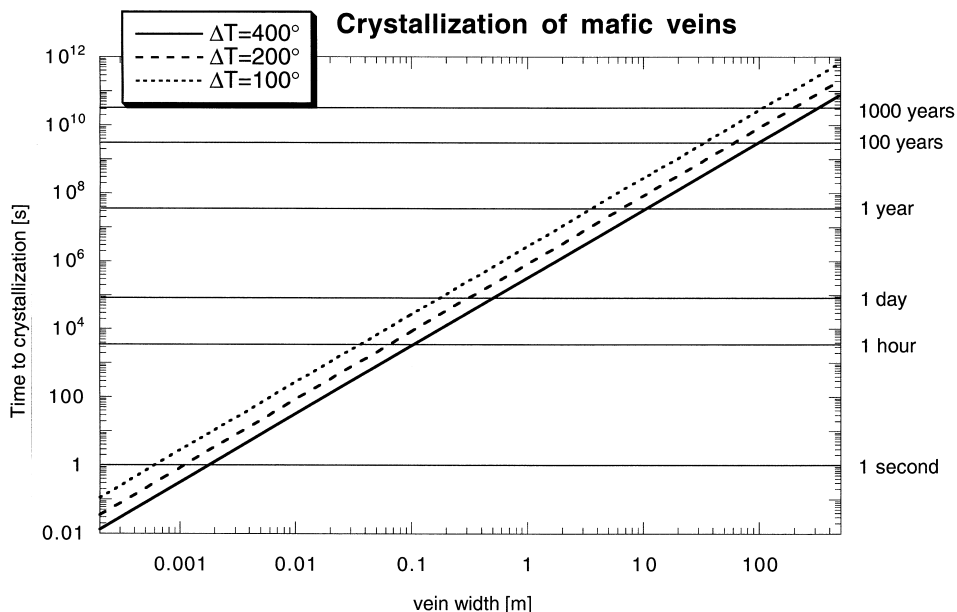
Fig. 6. Plot of crystallization time versus vein width contoured for temperature difference, ΔT between mafic veins and country rock. Curves calculated with eq. 4-143 of [39] for conductive cooling of a crystallizing vein. Average values for material parameters from the literature: latent heat of fusion $L = 300$ kJ kg^{-1}, heat capacity $C_p = 1.0$ kJ kg^{-1}°C^{-1}; thermal conductivity $k = 2.5$ W m^{-1}°C^{-1}; specific mass $\rho = 2.8 \times 10^3$ kg m^{-3}.
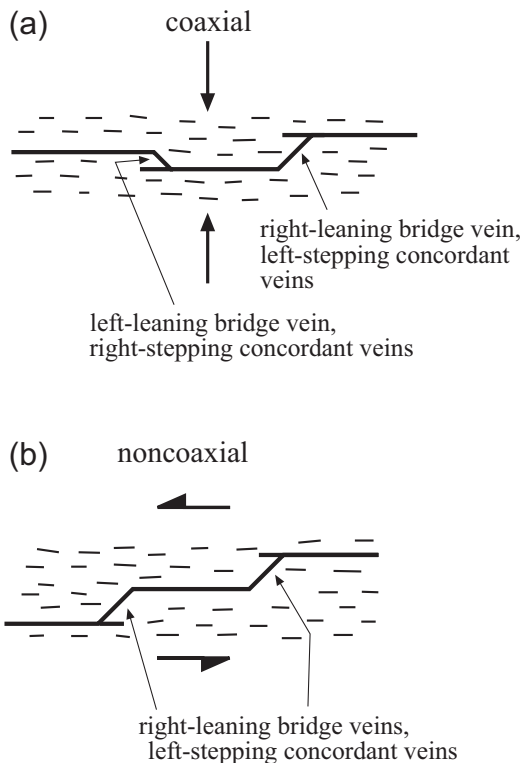
Fig. 7. Mafic vein arrays intruded during predominantly coaxial (a) and noncoaxial (b) shearing. Note orientation of bridge veins between concordant host veins and stepping sense of linked concordant mafic veins (see text for explanation). Veins (black) and mylonitic foliation in host rock (dashed). Plane of view is the XZ fabric plane.

For example, barbs extending parallel to the foliation from the outer margins of veins (Fig. 2b,c) can be interpreted as de-activated vein tips that were short-circuited or cut off from their concordant, host vein by the impinging tip of an adjacent vein (Fig. 5b,c). The rounded xenolith of mylonite in Fig. 3b (lower arrow) may have resulted from the linkage of two such curved vein tips ([35]: "rotated bridge" in their fig. 2).

Finally, both the leaning direction of bridge veins and the stepping-direction of concordant host veins can be used as qualitative indicators of syn-intrusive, kinematic vorticity in a given fabric plane (Fig. 7). For example, the almost equal abundance of right- and left-leaning bridge veins linking both right- and left-stepping concordant vein pairs in the Val Orasso

outcrop are consistent with independent structural evidence above for a strong component of coaxial strain during mylonitization. During purely coaxial shear (kinematic vorticity, $W_k = 0$), conjugate leaning directions of bridge veins that link right- and left-stepping concordant veins are expected to occur in all three principal finite strain surfaces (Fig. 7a). In contrast, during highly noncoaxial deformation (kinematic vorticity, $W_k \approx 1$), most bridge veins are expected to lean against the direction of shear (Fig. 7b), consistent with vein tip propagation through areas of tensile stress concentration asymmetrically distributed at opposite ends and sides of the host veins. The uniform-stepping sense of linked concordant host veins (e.g., left-stepping for sinistral simple shear in Fig. 7b) is similar, but not identical, to the en relais vein geometry proposed by Hanmer et al. ([42]: their fig. 10), in which the tips rather than the margins of the elongate host veins form parallel to the shearing plane. Both configurations are mechanically possible and probably reflect different ratios of melt pressure to lithostatic pressure (P_m/P_l) as well as the presence (in our case) of a strong mechanical anisotropy in the form of a pre-existing mylonitic foliation.

6. Implications for lower crustal structure and rheology

These results have broad implications for the mechanisms and conditions of melt transport in the lower continental crust, and also for the way in which magmatic underplating affects crustal structure and rheology. They confirm Holliger and Levander's [8] idea that mafic sills form in depth-intervals of the crust where the mechanical anisotropy is subhorizontal and when the effective normal stresses are zero or negative. However, there remains the classical chicken-or-the-egg-first dilemma of whether mylonitic deformation facilitated vein intrusion or vice versa. Both hypotheses have been proposed for the relationship between Early Permian deformation and magmatic underplating in the Ivrea–Verbano Zone: Rutter et al. [43] speculated that mafic melt from the Mafic Complex (Fig. 1) was injected as sills into mylonitically deforming metasediments (see their fig. 8a), whereas Quick et al. [44] conjectured that

hot, upwelling mafic intrusions within the Mafic Complex thermally weakened the adjacent metasediments, thereby facilitating the mylonitization that accommodated Early Permian crustal attenuation.

Although both scenarios are possible, the available evidence in the Ivrea–Verbano Zone, and especially at the CMB Line, indicates that localized, sporadic fracturing at low differential stress and high melt pressure along active shear zones strongly channeled the flow of mafic melt within the lower continental crust. Fracturing parallel rather than oblique to the foliation is common because mylonites are mechanically anisotropic (i.e., much weaker normal to foliation than in other directions) and because the melt pressure usually only slightly exceeds the lithostatic pressure. The good agreement of differential stress estimates from fracture criteria ($\leq$10–20 MPa) with those obtained from the extrapolation of experimental creep laws indicates that viscous and brittle deformation in the deep crust can occur simultaneously at very low differential stresses and at high temperatures provided that the pressure of the fluid (= mafic melt, in this case) locally exceeds the normal stress on the foliation ($\approx$ lithostatic pressure) for short periods of time.

The interconnection of veins containing slightly overpressurized, mafic melt parallel to a subhorizontal, mylonitic foliation like that in the IVZ allows rapid distribution of this melt within the lower crust. Veining on the scale of the continental crust is manifest in the IVZ by numerous, thick mafic veins with high length to width ratios that protrude from the Mafic Complex into the metasediments (Fig. 1). The rate and lateral extent of mafic veining in the continental crust depends primarily on the viscosity of the melt, the duration of melt overpressure, and the thermal state of the crust. Using the approach in the previous section, one can estimate that at a ΔT of 100–200°C (vein melt at 1000°C, granulite facies gneiss at 800–900°C, [45]) mafic veins with thicknesses (10–100 m) and lengths (100–1000 m) like those in the IVZ, and commonly inferred for the lower continental crust [8,46], crystallize after only several hundreds to thousands of years (Fig. 6). This time is very short compared to the 15–20 Ma duration of Early Permian crustal attenuation and magmatism in the IVZ [14,47], suggesting that the lateral propagation of syn-mylonitic mafic veins within the lower crust occurred episodically during mylonitization.

The impressive extent and rate of lateral vein propagation have implications for the tectonic interpretation of seismic reflection profiles of the lower continental crust. The originally subhorizontal mafic layers in the IVZ are sufficiently thick and have a large enough impedance contrast with the surrounding gneiss to generate laterally continuous seismic reflectors in synthetic seismic profiles of the IVZ [5,8,48]. Syn-mylonitic mafic sills are therefore a likely cause of the subhorizontal, laminar reflectivity observed in seismic sections of lower continental crust. Consequently, post-magmatic shearing of dikes [7], although certainly extant in some areas [4], is not necessary to explain the lateral continuity of lower crustal seismic reflectors.

If deep crustal mylonite zones are inclined, as the CMB Line may have been, they can also channel overpressurized melts from deep crustal melt chambers into intermediate crustal levels. In fact, there are no feeder dikes connecting the mafic veins along the CMB Line with cogenetic mafic and ultramafic rocks of the Mafic Complex in the IVZ. We therefore suspect that the CMB Line tapped some other, as yet unknown, mafic intrusive body that remains unexposed, or was eroded or faulted out during Alpine verticalization of the IVZ. We note that our observations do not support Holliger and Levander's [8] underplating model of the IVZ in which vertical dikes connect deep crustal magma chambers with sills higher in the crust. We are also unable to verify Brown and Solar's [49] contention that melt in active shear zones migrates parallel to the direction of principal finite strain. Rather, the structural relations along the CMB Line indicate that syn-mylonitic melt in a non-coaxial flattening environment probably intruded from the intermediate principal strain direction. Given the rapid flow of low viscosity mafic melts within propagating veins, one can reasonably predict that once veins link up to form conduits within the mylonitic foliation, overpressured melt will migrate down melt pressure gradients, irrespective of the orientation of the finite strain ellipsoid in the host mylonite. Therefore, the principal stretching direction in syn-intrusive mylonite does not necessarily indicate the melt transport direction in the shear zone.
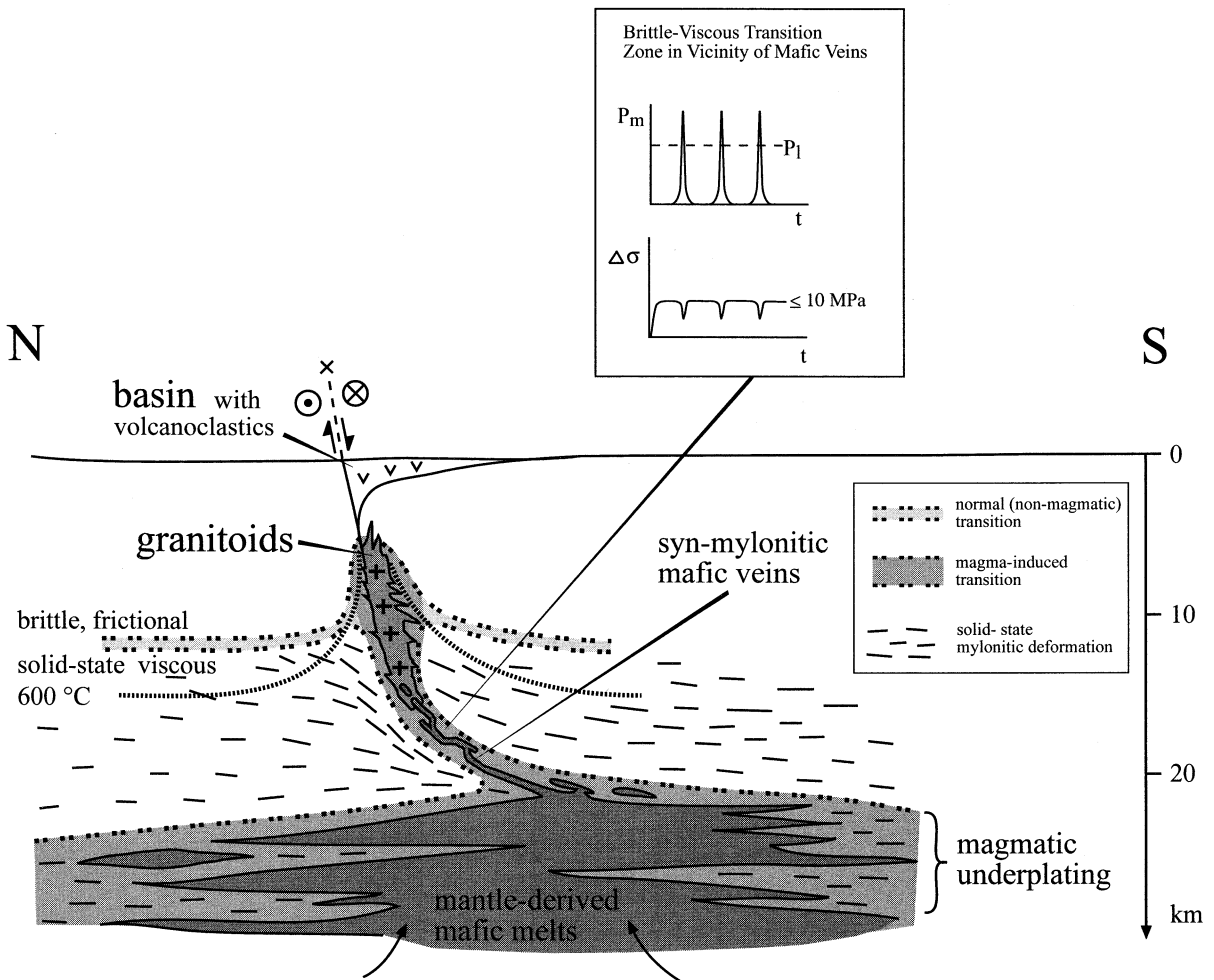
Fig. 8. Reconstructed cross section through magmatically underplated continental crust of the southern Alps in Early Permian time. Dashed lines = trace of mylonitic foliation, dark shaded area = mafic melt. Closely dotted line marks the 600°C isotherm corresponding approximately to fully viscous flow in quartz–feldspar rock undergoing dislocation creep at natural strain rates (10^{-10} to 10^{-14} s^{-1}). Double-dotted lines delimit lightly shaded depth interval of transient mechanical behavior marking the transition from brittle, frictional deformation to viscous flow. Inset shows fluctuations in melt pressure and differential stress within this depth interval (see text).

Fig. 8 depicts the salient structural and mechanical features of magmatically underplated crust as summarized below. The transport of hot mafic melt along active shear zones into cooler, intermediate crustal rock is predicted to have two main effects: First, melt thermally weakens the deforming rock, thereby increasing the strain rate and/or broadening and lengthening the shear zone. The effective viscosity of the CMB mylonite is estimated to have been about 10^{16}–10^{20} Pa s based on the low differential stresses (≤ 10–20 MPa) above for anatectic CMB

mylonite and average strain rates (10^{-10}–10^{-14} s^{-1}) for mylonite undergoing dislocation creep. Thermal weakening locally raises the depth of the brittle to viscous transition, but transient melt overpressure greatly increases the depth range of combined viscous and brittle deformation (shaded area between double-dotted lines in Fig. 8). Strength fluctuations associated with sporadic melt pulses and fracturing (Fig. 8, inset) are not restricted to narrow shear zones but are also expected to affect the entire magmatically underplated, mylonitic crust. Second, veined

mafic melt triggers partial melting of felsic country rock and back-veining of the resulting silica-rich melts into the mafic veins, as observed in the mylonitic gneisses of the CMB Line. Mingling and mixing of these back-veined melts derived from the country rock with the mafic melts can produce granitoids, a phenomenon observed along the CMB Line. Further ascent of mafic melt within intermediate crustal shear zones is limited by decreasing temperature and/or increasing density contrast of the mafic melt with the country rock. The former increases the viscosity of both the melt and the mylonitic country rock and eventually leads to entrapment of mafic melt within the shear zone, similar to the way in which some granitoid melts are thought to pond just below the brittle to viscous transition in the middle to upper crust [50]. These predictions could be checked with further investigation of magmatic rocks from various levels of exposed crustal cross sections in order to provide a better phenomenological basis for dynamic and thermal modelling.

Acknowledgements

References

[1] K. Furlong, D.M. Fountain, Continental crustal underplating: thermal considerations and seismic–petrologic consequences, J. Geophys. Res. 91 (8) (1986) 8285–8294.

[2] K.H. Olson, W.S. Baldridge, J.F. Callender, Rio Grande rift: an overview, Tectonophysics 143 (1987) 119–139.

[3] T.J. Reston, Evidence for shear zones in the lower crust offshore Britain, Tectonics 7 (1988) 929–945.

[4] A. Green, B. Milkereit, J. Percival, A. Davidson, R. Parrish, F. Cook, W. Geis, W. Cannon, D. Hutchinson, G. West, R. Clowes, Origin of deep crustal reflections: seismic profiling across high-grade metamorphic terranes in Canada, Tectonophysics 173 (1990) 627–638.

[5] L.D. Hale, G.A. Thompson, The seismic reflection character of the continental Mohorovicic discontinuity, J. Geophys. Res. 86 (B6) (1982) 4625–4635.

[6] D.M. Fountain, Implications of deep crustal evolution for seismic reflection seismology, in: M. Barazangi, L. Brown (Eds.), Reflection Seismology: The Continental Crust, Am. Geophys. Union, Geodyn. Ser. 14 (1986) 1–17.

[7] S. McGeary, M.R. Warner, Seismic profiling of the continental lithosphere, Nature 317 (1985) 795–797.

[8] K. Holliger, A. Levander, Structure and seismic response of extended continental crust: Stochastic analysis of the Strona–Ceneri and Ivrea zones, Geology 22 (1994) 79–82.

[9] J.D. Clemens, C.K. Mawer, Granitic magma transport by fracture propagation, Tectonophysics 204 (1992) 339–360.

[10] N. Petford, R.C. Kerr, J.R. Lister, Dike transport of granitoid magmas, Geology 21 (1993) 845–848.

[11] W.J. Collins, E.W. Sawyer, Pervasive granitoid transfer through the lower-middle crust during non-coaxial compressional deformation, J. Metamorphic Geol. 14 (1996) 565–579.

[12] S.M. Wickham, The segregation and emplacement of granitic magmas, J. Geol. Soc. London 144 (1987) 281–297.

[13] A. Boriani, L. Burlini, R. Sacchi, The Cossato–Mergozzo–Brissago Line and the Pogallo Line (Southern Alps, Northern Italy) and their relationships with the late-Hercynian magmatic and metamorphic events, Tectonophysics 182 (1990) 91–102.

[14] M.R. Handy, L. Franz, F. Heller, B. Janott, R. Zurbriggen, Multistage accretion, orogenic stacking and exhumation of continental crust (southern Alps, Italy and Switzerland), submitted to Tectonics.

[15] A. Zingg, M.R. Handy, J.C. Hunziker, S.M. Schmid, Tectonometamorphic history of the Ivrea Zone and its relation to the crustal evolution of the Southern Alps, Tectonophysics 182 (1990) 169–192.

[16] L. Pinarelli, A. Del Moro, A. Boriani, Rb–Sr geochronology of Lower Permian plutonism in Massicio dei Laghi, Southern Alps (NW-Italy), Rend. Soc. It. Mineral. Petrol. 43 (2) (1988) 411–428.

[17] M.R. Handy, A. Zingg, The tectonic and rheologic evolution of an attenuated cross section of the continental crust: Ivrea crustal section, southern Alps, northwestern Italy and southern Switzerland, Geol. Soc. Am. Bull. 103 (1991) 236–253.

[18] S.M. Schmid, A. Zingg, M.R. Handy, The kinematics of movements along the Insubric Line and the emplacement of the Ivrea Zone, Tectonophysics 135 (1987) 47–66.

[19] G. Rivalenti, A. Rossi, F. Siena, S. Sinigoi, The Layered Series of the Ivrea–Verbano Igneous Complex, Western Alps, Italy, Tschermaks Mineral. Petrogr. Mitt. 33 (1984) 77–99.

[20] S. Sinigoi, J. Quick, D. Clemens-Knott, A. Mayer, G. Demarchi, Chemical evolution of a large mafic intrusion in

the lower crust, Ivrea–Verbano Zone, J. Geophys. Res. 99 (11) (1994) 21575–21590.

[21] A. Boriani, V. Caironi, E. Giobbi Origoni, R. Vannucci, The Permian intrusive rocks of Serie dei Laghi (Western Southern Alps), Acta Vulcanol. 2 (1992) 73–86.

[22] M.B. Wolf, P.J. Wyllie, Dehydration melting of amphibolite at 10 kbar: the effects of temperature and time, Contrib. Mineral. Petrol. 115 (1994) 369–383.

[23] L. Franz, S. Teufel, O. Oncken, Thermische Entwicklung der Ivrea- und Strona–Ceneri-Zone (N-Italien), Terra Nostra 96 (2) (1996) 58–60.

[24] R.H. Sibson, A note on fault reactivation, J. Struct. Geol. 7 (6) (1985) 751–754.

[25] R. Kerrich, Fluid infiltration into fault zones: chemical, isotopic and mechanical effects, Pure Appl. Geophys. 124 (12) (1986) 225–268.

[26] J.W. Cosgrove, The influence of mechanical anisotropy on the behaviour of the lower crust, Tectonophysics 280 (12) (1997) 1–15.

[27] D.T. Secor, Role of fluid pressure in jointing, Am. J. Sci. 263 (1965) 633–646.

[28] M.A. Etheridge, Differential stress magnitudes during regional deformation and metamorphism: Upper bound imposed by tensile fracturing, Geology 11 (1983) 231–234.

[29] M.A. Etheridge, V.J. Vall, R.H. Vernon, The role of the fluid phase during regional metamorphism and deformation, J. Metamorphic Geol. 1 (1983) 205–226.

[30] J.E. Streit, S.F. Cox, Fluid infiltration and volume change during mid-crustal mylonitization of Proterozoic granite, King Island, Tasmania, J. Metamorphic Geol. 16 (1998) 197–212.

[31] D.L. Kohlstedt, B. Evans, S.J. Mackwell, Strength of the lithosphere: Constraints imposed by laboratory experiments, J. Geophys. Res. 100 (B9) (1995) 17587–17602.

[32] J.E. Olson, D.D. Pollard, The initiation and growth of en échelon veins, J. Struct. Geol. 13 (5) (1991) 595–608.

[33] D.D. Pollard, P. Segal, Theoretical displacements and stresses near fractures in rock: with applications to faults, joints, veins, dikes, and solution surfaces, in: B.K. Atkinson (Ed.), Fracture Mechanics of Rock, Academic Press, London, 1987, pp. 277–349.

[34] D.D. Pollard, P. Segall, P.T. Delaney, Formation and interpretation of dilatant échelon cracks, Geol. Soc. Am. Bull. 93 (1982) 1291–1303.

[35] R. Nicholson, D.D. Pollard, Dilation and linkage of échelon cracks, J. Struct. Geol. 7 (5) (1985) 583–590.

[36] P. Lin, J.M. Logan, The interaction of two closely spaced cracks: a rock model study, J. Geophys. Res. 96 (B13) (1991) 21667–21675.

[37] M.R. Hempton, K. Neher, Experimentally produced deformation above en échelon strike-slip faults, J. Struct. Geol. 8 (6) (1986) 597–605.

[38] S.D. Hallam, M.F. Ashby, Compressive brittle fracture and the construction of multi-axial failure maps, in: D.J. Barber, P.G. Meredith (Eds.), Deformation in Minerals, Ceramics and Rocks, The Mineralogical Society Series 1 (1990) 84–108.

[39] D.L. Turcotte, G. Schubert, Geodynamics: Applications of Continuum Physics to Geological Problems, Wiley, New York, 1982, 450 pp.

[40] B.K. Atkinson, P.G. Meridith, The theory of subcritical crack growth with applications to minerals and rocks, in: B.K. Atkinson (Ed.), Fracture Mechanics of Rock, Academic Press, London, 1987, pp. 111–166.

[41] A. Escher, S. Jack, J. Watterson, Tectonics of the North Atlantic Proterozoic dyke swarm, Philos. Trans. R. Soc., London A 280 (1976) 529–539.

[42] S. Hanmer, F. Mengel, J. Connelly, J. van Gool, Significance of crustal scale shear zones and synkinematic mafic dikes in the Nagssugtoqidian orogen, SW Greenland: a re-examination, J. Struct. Geol. 19 (1) (1997) 59–75.

[43] E.H. Rutter, K.H. Brodie, P.J. Evans, Structural geometry, lower crustal magmatic underplating and lithospheric stretching in the Ivrea–Verbano zone, northern Italy, J. Struct. Geol. 15 (345) (1993) 647–662.

[44] J.E. Quick, S. Sinigoi, A. Mayer, Emplacement dynamics of a large mafic intrusion in the lower crust, Ivrea–Verbano Zone, northern Italy, J. Geophys. Res. 99 (B11) (1994) 21559–21573.

[45] A. Zingg, The Ivrea and Strona–Ceneri Zones (Southern Alps, Ticino and N-Italy) — a review, Schweiz. Mineral. Petrogr. Mitt. 63 (1983) 361–392.

[46] K. Fuchs, On the properties of deep crustal reflectors, Z. Geophys. 35 (1969) 133–149.

[47] A. Henk, L. Franz, S. Teufel, O. Onken, Magmatic underplating, extension, and crustal reequilibration: Insights from a cross-section through the Ivrea Zone and Strona-Ceneri Zone, Northern Italy, J. Geol. 105 (1997) 367–377.

[48] M.M. Burke, D.M. Fountain, Seismic properties of rocks from an exposure of extended continental crust — new laboratory measurements from the Ivrea Zone, Tectonophysics 182 (1990) 119–146.

[49] M. Brown, G.S. Solar, Shear-zone systems and melts: feedback relations and self-organization in orogenic belts, J. Struct. Geol. 20 (23) (1998) 211–227.

[50] B. Kriens, B. Wernicke, Characteristics of a continental margin magmatic arc as a function of depth: the Skagit–Methow crustal section, in: M.H. Salisbury, D.M. Fountain (Eds.), Exposed Cross-Sections of the Continental Crust, Kluwer, Dordrecht, NATO ASI Series C 317 (1990) 159–174.